

TWO PROBABILISTIC ALGORITHMS FOR MEG/EEG SOURCE RECONSTRUCTION

Johanna M. Zumer^{1,2}, Hagai T. Attias³, Kensuke Sekihara⁴, Srikantan S. Nagarajan^{1,2}

¹ Biomagnetic Imaging Lab, Dept. of Radiology, UCSF, San Francisco, CA, 94143-0628 USA

² Joint Graduate Group in Bioengineering, UCSF/UC Berkeley, San Francisco, CA, 94143-0628 USA

³ Golden Metallic, Inc., San Francisco, CA, 94147, USA

⁴ Dept. of Systems Design and Engineering, Tokyo Metropolitan University, Tokyo, 191-0065 Japan

ABSTRACT

We have developed two algorithms for source imaging from MEG/EEG data. Contribution to sensor data from a source at a particular voxel is expressed as the product of a known lead field and temporal basis functions with unknown coefficients. Temporal basis functions are in turn estimated from data. The first algorithm models activity outside the voxel of interest by a full-rank covariance matrix and estimates unknowns by maximizing the likelihood. The second algorithm parameterizes activity outside the voxel of interest as a linear mixture of a set of unknown Gaussian factors plus Gaussian sensor noise and estimates all unknown quantities using an Expectation-Maximization (EM) algorithm. In both cases, the source image map is the likelihood of a dipole source at each voxel. Performance in simulations and real data demonstrate significant improvement over existing source localization methods.

1. INTRODUCTION

Magnetoencephalography (MEG) and electroencephalography (EEG) are popular methods of noninvasively measuring the spatiotemporal characteristics of human neural activity. Both techniques record the effects of neural activity at the scalp with millisecond precision. Arrays of MEG sensors detect femtoTesla changes in the magnetic field outside the head; arrays of EEG sensors measure the corresponding voltage potential changes on the scalp. The increasing availability of whole-head MEG/EEG sensor arrays allows for higher-resolution spatiotemporal reconstruction of neural activity, thus increasing the demand for improved methods for source reconstruction.

All source localization techniques, which can be broadly classified as parametric or tomographic, make assumptions to overcome the ill-posed inverse problem. Parametric methods, including equivalent current dipole (ECD) fitting techniques, assume knowledge about the number of sources and their approximate locations. A single dipolar source can be localized well, but ECD techniques poorly describe multiple sources or

The authors would like to thank Kenneth Hild and Sarang Dalal for helpful discussions, and NIH R01NS44590 and NIH R01DC004855 for support.

sources with large spatial extent. Alternatively, tomographic methods reconstruct an estimate of source activity at every grid point across the whole brain. Specifically, the adaptive beamformer has been shown to have the best spatial resolution and zero localization bias [1]. However, beamformers are very sensitive to highly temporally-correlated sources [2].

This paper presents a probabilistic modeling framework for dipole source localization. Two techniques based on this framework are described and demonstrated. Each technique uses a probabilistic hidden variable model that describes the observed sensor data in terms of activity from unobserved brain and interference sources. The unobserved source activities and model parameters are inferred from the data by an Expectation-Maximization algorithm. These techniques create an image of brain activity by scanning the brain, inferring the models from sensor data, and using them to compute the likelihood of a dipole at each voxel.

2. METHODS

The probabilistic models in this paper are based on a physical description of neural activity, in which brain sources are modeled by current dipoles. For a given volume conductor model, the $K \times 3$ forward lead field matrix $F(r)$ represents the physical relationship between a dipole at voxel r and its influence on sensor $k = 1 : K$ [3]. In both models, we assume the source activity is a linear combination of $J \times N$ temporal basis functions ϕ computed from the data as described in Section 2.3, spatially weighted at each voxel by a $3 \times J$ dipole mixing matrix $G(r)$. We compute the maximum likelihood at each voxel; the spatial peaks of this likelihood map correspond to the most likely source locations.

2.1. Model 1

In Model 1, we describe a generative model for the $K \times 1$ sensor data y_n :

$$y_n = F(r)G(r)\phi_n + w_n(r) \quad (1)$$

The noise $w_n(r)$ is modeled by zero-mean Gaussian with

a general $K \times K$ precision matrix Λ . Both the parameters G and Λ are unknown. For a large number of sensors K , the precision matrix becomes quite large and difficult to infer accurately from the data. It may also become ill-conditioned. Hence, we place a prior Wishart distribution on the precision matrix:

$$p(\Lambda) = W(\Lambda|\nu, \Sigma_0) \propto |\Lambda|^{\nu/2} e^{-\frac{1}{2}Tr\Sigma_0\Lambda} \quad (2)$$

where Σ_0 and ν are hyperparameters. We choose $\nu = K + 2$ for the distribution to be normalizable and $\Sigma_0 = \Lambda_0^{-1} + \sigma$, where σ is diagonal with $\sigma_{ii} = \max(\sum_n y_{in}^2/N - (\Lambda_0^{-1})_{ii}, 0)$ and calculation of Λ_0^{-1} is described in Section 2.3.

For each scanned voxel, we consider the likelihood function:

$$\mathcal{L}(r) = \log p(y|\Lambda) + \log p(\Lambda) \quad (3)$$

The model parameters $G(r)$ and $\Lambda(r)$ are inferred from the data by maximizing $\mathcal{L}(r)$, leading to the following (dropping the dependence on voxel r for clarity):

$$G(r) = (F^T S^{-1} F)^{-1} F^T S^{-1} R_{y\phi} R_{\phi\phi}^{-1} \quad (4)$$

$$\Lambda^{-1}(r) = \frac{1}{N + \nu - K - 1} (R_{yy} - FGR_{\phi y} - R_{y\phi}G^T F^T + FGR_{\phi\phi}G^T F^T + \Sigma_0) \quad (5)$$

where

$$S = \frac{1}{N + \nu - K - 1} (R_{yy} - R_{y\phi}R_{\phi\phi}^{-1}R_{\phi y} + \Sigma_0) \quad (6)$$

$$R_{yy} = \sum_{n=1}^N y_n y_n^T, \quad R_{y\phi} = \sum_{n=1}^N y_n \phi_n^T, \quad R_{\phi\phi} = \sum_{n=1}^N \phi_n \phi_n^T \quad (7)$$

The maximized likelihood is then:

$$\mathcal{L}(r) = \frac{N + \nu - K - 1}{2} \log|\Lambda(r)| + \text{const.} \quad (8)$$

whose spatial peaks correspond to the most likely source locations.

This model and its solution are related to that proposed by Dogandzic and Nehorai [4] and Baryshnikov et al. [5]. We modify their work by precomputing the basis functions from the data (see Section 2.3) and by placing a prior Wishart distribution on the full-rank precision matrix.

2.2. Model 2

In contrast to Model 1, we now more explicitly model those contributions to sensor measurements not arising from a dipole source at the voxel r . The $L \times 1$ unknown interference factors $x_n(r)$ correspond to activity in all voxels excluding r , A is a $K \times L$ unknown mixing matrix, and the sensor noise has

unknown diagonal precision λ . The corresponding generative model for sensor data is:

$$y_n = F(r)G(r)\phi_n + A(r)x_n(r) + v_n(r) \quad (9)$$

To complete specification of the model, we have:

$$p(y_n|x_n, A, \lambda) = \mathcal{N}(y_n|FG\phi_n + Ax_n, \lambda) \quad (10)$$

$$p(x_n) = \mathcal{N}(x_n|0, I), \quad p(v_n) = \mathcal{N}(v_n|0, \lambda) \quad (11)$$

Notice that in place of the $(K^2 + K)/2$ elements of the precision matrix Λ in Model 1, we now infer from the data just the $KL + K$ elements of A and λ . Since typically $L \ll K$ (in our case $K = 275$ and $L \sim 10$), Model 2 has significantly less parameters and can thus be inferred more accurately.

We use an expectation-maximization (EM) algorithm to infer the unknown quantities from the data. EM is an iterative algorithm for inferring probabilistic models with hidden variables from data. Each EM iteration has an E-step and an M-step. The E-step computes the posterior distribution $p(x_n|y_n)$ over the hidden variables x_n and the M-step updates the parameters G, A, λ . EM algorithms iteratively maximize the data likelihood under the model; their convergence is guaranteed. Specifically, in the E-step, we update:

$$\begin{aligned} \bar{x}_n &= \Gamma^{-1} A^T \lambda A y_n \\ \Gamma &= A^T \lambda A + I \\ p(x_n|y_n) &= \mathcal{N}(x_n|\bar{x}_n, \Gamma) \end{aligned} \quad (12)$$

and, in the M-step, we update:

$$G(r) = (F^T \lambda F)^{-1} F^T \lambda (R_{y\phi} - R_{yx} R_{xx}^{-1} R_{x\phi}) (R_{\phi\phi} - R_{\phi x} R_{xx}^{-1} R_{x\phi})^{-1} \quad (13)$$

$$A(r) = (R_{yx} - FGR_{\phi x}) R_{xx}^{-1} \quad (14)$$

$$\lambda(r) = N [\text{diag}(R_{y'y'} - AR_{y'x})]^{-1} \quad (15)$$

$$y'_n(r) = y_n - F(r)G(r)\phi_n \quad (16)$$

We have omitted expressions for $R_{yx}, R_{y'x}, R_{\phi x}$ and R_{xx} for lack of space. The maximized likelihood function for this model is:

$$\mathcal{L}(r) = \frac{N}{2} \log \frac{|\lambda/2\pi|}{|\Gamma|} - \frac{1}{2} \sum_{n=1}^N (y_n'^T \lambda y_n' - \bar{x}_n^T \Gamma \bar{x}_n) \quad (17)$$

2.3. Computing temporal basis functions from data

We assume that the neural activity at all possible source locations can be described as a linear combination of temporal basis functions. To estimate these basis functions from the data, we use a variant of a factor analysis (FA) model to describe the sensor data as:

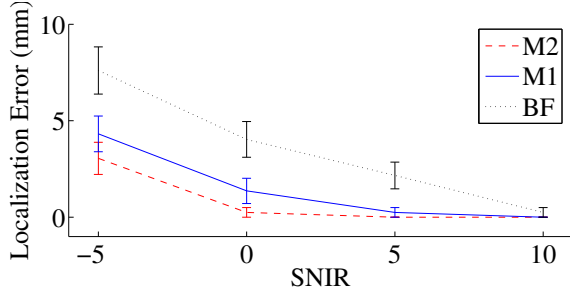


Fig. 1. Localization error distribution for single randomly-placed source for Model 1 (M1), Model 2 (M2), and beamforming (BF), as a function of SNIR. Error bars represent the standard error of the mean.

$$y_n = B\phi_n + u_n \quad (18)$$

The J -dimensional factors ϕ_n are modeled with a prior probability distribution of zero-mean Gaussian with diagonal unit precision. The noise term u_n is modeled by a zero-mean Gaussian with a known precision matrix Σ (see below). We use EM to infer the posterior mean of ϕ_n and the mixing matrix B . In the E-step, we update:

$$\phi_n = (B^T \Sigma B + I)^{-1} B^T \Sigma y_n \quad (19)$$

In the M-step, we update:

$$B = R_{y\phi} R_{\phi\phi}^{-1} \quad (20)$$

We now discuss the choice of Σ . The work described in this paper uses the evoked stimulus experimental paradigm: each trial consists of a prestimulus period and a poststimulus period, separated by the stimulus onset. The poststimulus sensor data arise from sources evoked by the stimulus, plus sources that were active prestimulus. Since here we are interested in localizing evoked sources, we use u_n in equation (18) to denote prestimulus signals. Hence, Σ is their precision matrix. Whereas it could be inferred by directly measuring the sample covariance, we choose to use a FA based technique: Writing $u_n = B_0 u'_n + v'_n$ where v'_n is noise with diagonal precision Λ_0 , we infer B_0 and Λ_0 by EM and set $\Sigma = (B_0 B_0^T + \Lambda_0^{-1})^{-1}$. A similar method was used in [6].

2.4. Simulations

The proposed methods were tested in a variety of realistic source configurations reconstructed on a 5mm voxel grid. A single-shell spherical volume conductor model was used to calculate the forward lead field [3]. Simulated datasets were constructed by using 700 samples of real MEG sensor data averaged over 100 trials collected while the subject was alert but not performing tasks or receiving stimuli. This background data thus includes sensor noise plus “ongoing” brain activity

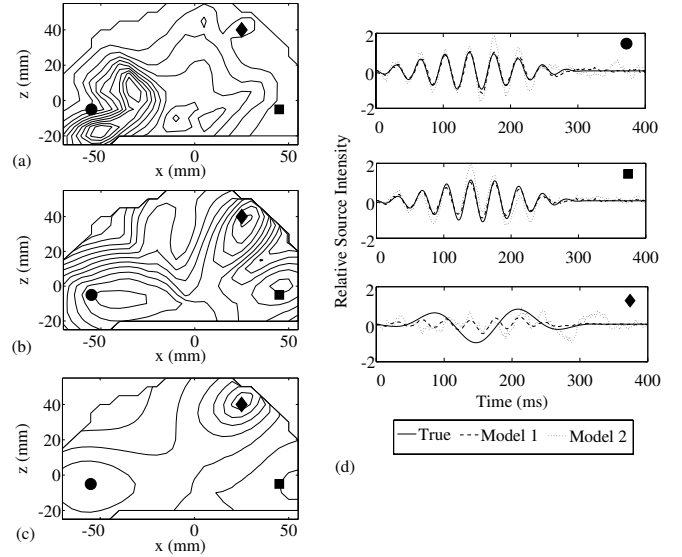


Fig. 2. Simulated circle and square sources are highly correlated ($\rho = 0.97$), while the diamond source is uncorrelated with the other two. (a) Beamformer power map. (b) Model 1 likelihood map. (c) Model 2 likelihood map. (d) Estimated time courses from the three sources.

that could interfere with evoked sources and adds spatial correlation to the sensor data. Gaussian-damped sinusoidal time courses are then placed at specific locations inside a voxel grid based on realistic head geometry. Their activity is projected onto the sensors for the “poststimulus” period only (the latter 400 samples) and added to the real background data. We define the Signal to Noise-plus-Interference Ratio (SNIR) as:

$$\text{SNIR} = 10 \log_{10} \frac{\sum_{k=1}^K \sum_{n=1}^N y_s^2}{\sum_{k=1}^K \sum_{n=1}^N y_b^2} \quad (\text{dB}) \quad (21)$$

where y_s is the sensor data from the sinusoidal sources only and y_b is the background data only.

2.5. Real data

Stimulus-evoked data was collected in a 275-channel CTF Systems MEG device from a healthy subject, who gave written consent prior to participation according to institutional review board approval. The stimulus was a noise burst presented binaurally in 120 trials.

3. RESULTS

3.1. Simulations

In the first set of simulations, a single source was placed randomly within a realistic head volume at 4 levels of SNIR. The plot of the mean localization errors of the likelihood maps are

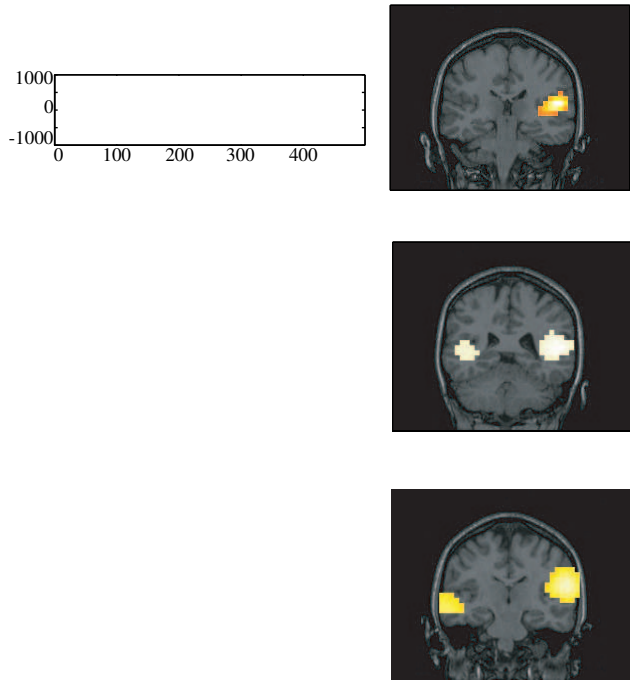


Fig. 3. Performance of models applied to real auditory MEG dataset. **(a)** (Right) Beamformer power map reconstructs only right auditory response. (Left) Beamformer estimated time course of right localization. **(b)** (Right) Likelihood map from Model 1 shows both right and left auditory peaks. (Left) Estimated time courses from Model 1 from both right and left auditory peaks. **(c)** (Right) Likelihood map from Model 2 shows both right and left auditory peaks. (Left) Estimated time courses from Model 2 from both right and left auditory peaks.

shown in Fig. 1. Even at the lowest SNIR of -5, Models 1 and 2 localized the source to within 5mm error, which, for real data, is on the order of the error due to coregistration of MEG data with the subject’s MRI. For all values of SNIR, Models 1 and 2 resulted in reduced error compared to an adaptive beamformer; the additional modeling of interference factors in Model 2 allowed for further improvement in localization.

Next, three sources were placed in realistic positions representing right somatosensory (rS1), right auditory (rA1), and left auditory (lA1) cortex. The temporal correlation between rA1 and lA1 was set at $\rho = 0.97$, while rS1 was uncorrelated with rA1 and lA1. As seen in Fig. 2, the likelihood maps of Models 1 and 2 are able to resolve all three sources, whereas the adaptive beamformer fails to find rA1 and includes spurious sources near the center of the head. Fig. 2 also shows the estimates of the time course for the three sources from Models 1 and 2. Two of the three sources are estimated very well, while the third includes some crosstalk.

Finally, we tested these models on the real auditory stimu-

lus dataset. Bilateral auditory evoked responses typically are highly temporally-correlated with each other. Fig. 3 shows the beamformer unable to find the left auditory response, whereas Models 1 and 2 clearly localize both left and right auditory cortex. All of the estimated time courses show the characteristic auditory peak around 100ms.

4. DISCUSSION

Two methods are introduced which localize stimulus-evoked MEG/EEG sources and estimate their temporal activity in a probabilistic framework. Both model the sources as a linear combination of temporal basis functions derived from the data using a factor analysis method. The methods have reduced localization error relative to beamforming and are not hampered by correlated sources. Additionally, the number or location of sources do not need to be specified, as in a standard dipole fitting method. Thus, these methods have clear advantages over current standard methods.

We derive equations and show results for MEG data only, although they could be easily extended for EEG data. The use of a probabilistic model framework allows inclusion of prior information, potentially from other modalities, to influence the solution.

5. REFERENCES

- [1] K. Sekihara, M. Sahani, and S.S. Nagarajan, “Localization bias and spatial resolution of adaptive and non-adaptive spatial filters for MEG source reconstruction,” *NeuroImage*, vol. 25, pp. 1056–1067, 2005.
- [2] K. Sekihara, S.S. Nagarajan, D. Poeppel, and A. Marantz, “Performance of an MEG adaptive-beamformer technique in the presence of correlated neural activities: Effects on signal intensity and time-course estimates,” *IEEE Trans Biomed Eng*, vol. 49, pp. 1534–1546, 2002.
- [3] J. Sarvas, “Basic mathematical and electromagnetic concepts of the biomagnetic inverse problem,” *Phys Med Biol*, vol. 32, pp. 11–22, 1987.
- [4] A. Dogandzic and A. Nehorai, “Estimating evoked dipole responses in unknown spatially correlated noise with EEG/MEG arrays,” *IEEE Trans. Sig. Proc.*, pp. 13–25, 2000.
- [5] B. V. Baryshnikov, B. D. Van Veen, and R. T. Wakai, “Maximum likelihood dipole fitting in spatially colored noise,” *Neurol Clin Neurophysiol*, vol. 2004, pp. 53–53, 2004.
- [6] S.S. Nagarajan, H.T. Attias, K.E. Hild, and K. Sekihara, “A graphical model for estimating stimulus-evoked brain responses from magnetoencephalography data with large background brain activity,” *NeuroImage*, 2006 [in press].